PHYSICAL REVIEW B

CONDENSED MATTER AND MATERIALS PHYSICS

THIRD SERIES, VOLUME 60, NUMBER 24 15 DECEMBER 1999-II

RAPID COMMUNICATIONS

Rapid Communications are intended for the accelerated publication of important new results and are therefore given priority treatment both in the editorial office and in production. A Rapid Communication in **Physical Review B** *may be no longer than four printed pages and must be accompanied by an abstract. Page proofs are sent to authors.*

Local field effects in optical excitations of semicore electrons

E. E. Krasovskii and W. Schattke

Institut für Theoretische Physik, Christian-Albrechts-Universität, Leibnizstrasse 15, D-24118 Kiel, Germany

(Received 11 October 1999)

We have calculated the dielectric matrix for $SrTiO_3$ and $BaTiO_3$ perovskites and for Nb metal by the extended linear augmented plane wave–**kp** method. Dipole-allowed transitions from localized semicore states generate strong local fields, which shift the optical absorption band arising from the semicore excitations to higher energies by several eV from the position suggested by one-electron energy differences. In the far UV range, the neglect of local field effects leads to dramatically overestimated values of reflectivity and absorbance. [S0163-1829(99)52048-1]

The ultraviolet spectroscopy has been a powerful tool to probe the electronic structure of solids.[1,2] The unambiguous interpretation of the experimental data requires calculations of optical absorption and reflection spectra from first principles. A way to perform such calculations is offered by the random-phase approximation (RPA),[3] which connects the dielectric matrix $\varepsilon_{\mathbf{GG}'}(\mathbf{q},\omega)$ to a one-electron energy band structure,[4]

$$\varepsilon_{\mathbf{GG}'}(\mathbf{q},\omega) = \delta_{\mathbf{GG}'} - \frac{e^2}{4\pi^2|\mathbf{q}+\mathbf{G}|\ |\mathbf{q}+\mathbf{G}'|}\sum_{\lambda\lambda'}\int_{BZ} d\mathbf{k} \times \frac{\langle \mathbf{k}+\mathbf{q}\lambda'|e^{i(\mathbf{q}+\mathbf{G}')\mathbf{r}}|\mathbf{k}\lambda\rangle\langle\mathbf{k}\lambda|e^{-i(\mathbf{q}+\mathbf{G})\mathbf{r}}|\mathbf{k}+\mathbf{q}\lambda'\rangle}{E_{\lambda'}(\mathbf{k}+\mathbf{q})-E_{\lambda}(\mathbf{k})-\hbar\omega+i\hbar\eta}. \quad (1)$$

Here $\mathbf{q}$ is the wave vector of the macroscopic field, $\mathbf{G}$ and $\mathbf{G}'$ are reciprocal lattice vectors, and $E_\lambda(\mathbf{k})$ and $|\mathbf{k}\lambda\rangle$ are band energies and eigenstates. The summation runs through occupied λ and unoccupied λ' states. The optical response of a crystal is determined by the long-wavelength limit of the macroscopic DF $\varepsilon(\mathbf{q},\omega)$, which is given by the matrix inverse of $\varepsilon_{\mathbf{GG}'}$,

$$\varepsilon(\omega) = \lim_{q\to 0}\frac{1}{[\varepsilon^{-1}]_{00}(\mathbf{q},\omega)}.$$

The element ε_{00} of the dielectric matrix is most important; its contribution to the macroscopic DF can be separated using the matrix identity[5]

$$\varepsilon = \varepsilon_{00} - \sum_{\mathbf{GG}'\neq 0}\varepsilon_{0\mathbf{G}'}[S^{-1}]_{\mathbf{GG}'}\varepsilon_{\mathbf{G}0}, \quad (2)$$

where S is a submatrix of ε restricted to $\mathbf{G},\mathbf{G}'\neq 0$. The effect of the full matrix is referred to as the local field (LF) correction $\Delta\varepsilon_{\mathrm{LF}} = \varepsilon - \varepsilon_{00}$.

In interpreting optical measurements it is usually assumed that the local field effects are small.[2,6] Then, strong dipole-allowed transitions are immediately recognized as peaks in optical absorption spectra $\mu(\omega) = (\sqrt{2}\omega/c)\sqrt{|\varepsilon(\omega)| - \mathrm{Re}\,\varepsilon(\omega)}$, and the energy positions of the peaks are thought to give the energies of the electronic excitations.

In this paper, we study the influence of local fields on the shape of absorption and reflection spectra. It can be stated *a priori* that in the case of dipole-allowed transitions between localized states, the LF corrections should be included. For transitions, say, between semicore Ba $5p$ and unoccupied $5d$ states, the magnitude of the density matrix elements for small $\mathbf{G}$ vectors is easy to estimate. Owing to the spatial localization of the $5p$ states, the matrix element $\langle 5d|\exp(i\mathbf{G}\mathbf{r})|5p\rangle/G$ can be approximated by an integral over a sphere surrounding the Ba atom:

$$\frac{4\pi i}{G}\int \psi^*_{5d}(\mathbf{r})j_1(Gr)\psi_{5p}(\mathbf{r})\sum_m Y^*_{1m}(\hat{G})Y_{1m}(\hat{r})d\mathbf{r}.$$

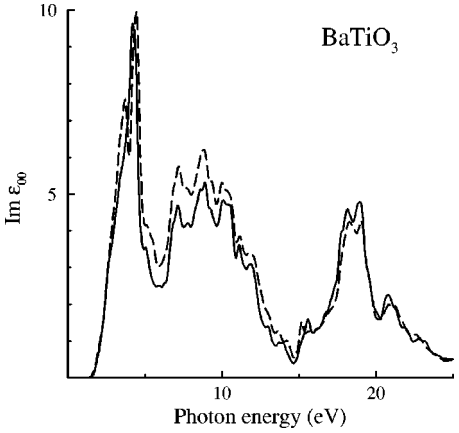

FIG. 1. Imaginary part of the element ε_{00} of the dielectric matrix of $BaTiO_3$. Solid line: momentum matrix elements (MME) are calculated from original all-electron wave functions. Dashed line: MME are calculated from the plane-wave decomposition of gouged wave functions. The maximum at 18.5 eV results form the transitions from Ba $5p$ semicore band located at -10 eV to Ba $5d$ resonance centered at 8.5 eV (energies are relative to the valence band maximum).

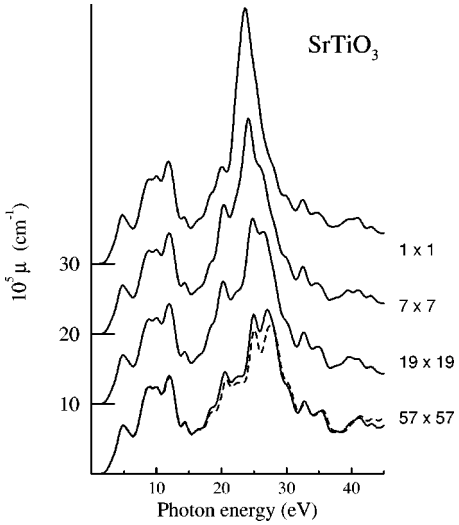

FIG. 2. Convergence of the absorption coefficient spectrum of $SrTiO_3$ with increasing the rank of the dielectric matrix. The upper curve does not include the LF corrections; the maximum at 23.5 eV in this curve reflects the transitions from Sr $4p$ semi-core band located at -14.5 eV to Sr $4d$ resonance centered at 8.5 eV. For the dielectric matrix of size 57×57 a pure RPA result is shown by the dashed line.

Only the term $l=1$ in the Rayleigh decomposition of the plane wave survives, and no selection rules additional to the dipole ones are introduced. The only difference to the dipole matrix element is the radial operator $j_1(Gr)/G$ instead of the dipole operator $r/3$, which is the $G\rightarrow0$ limit of $j_1(Gr)/G$. The localization radius of $5p$ states is ~3 a.u. In that range the function $j_1(Gr)/G$ is smaller than $r/3$ by not more than a factor of 2. The same estimate is valid for $s\rightarrow p$ and $d\rightarrow p$ transitions. Thus, the microscopic fields associated with semicore excitations are not negligible in comparison with the bare diagonal response, and *ab initio* calculations of the full dielectric matrix are necessary to describe optical absorption in the UV range.

The macroscopic dielectric function has been extensively studied using *ab initio* methods of band theory.[7–14] Most of the studies were devoted to the wave-vector dependence of the energy loss spectra; optical properties were considered in Refs. 10–14 (see also references in Ref. 11). The authors did not observe a strong influence of the local fields on the optical spectra. The loss function $-\mathrm{Im}[\varepsilon(\mathbf{q},\omega)]^{-1}$ is, however, very sensitive to small changes in $\varepsilon(\mathbf{q},\omega)$; indeed, the LF corrections were found important for the loss function.[8,9,11] Aryasetiawan and co-workers recognized an important role of core electrons in generating the local fields and discussed the implications for the plasmon dispersion.[8,9]

In the majority of the calculations of the dielectric matrix, a pseudopotential plane-wave formalism is used, e.g., in Refs. 12–14. Only a few all-electron calculations have been reported: with the modified augmented plane-wave method by Bross and co-workers,[10,11] and with the linear muffin-tin orbital method within the atomic sphere approximation by Aryasetiawan and co-workers.[7–9]

In the present study we employ the extended linear augmented plane wave (ELAPW)-**kp** method.[15] The **kp** formalism reduces the **k**-point dependence of the APW basis set to a multiplication of the APW's with a reference Bloch vector $\mathbf{k}_0$ by the function $\exp[i(\mathbf{k}-\mathbf{k}_0)\mathbf{r}]$. Thus, the time-consuming operations of setting up the Hamiltonian, overlap, and momentum matrices are performed only once for a given crystal potential. For the calculation of the dielectric matrix, it is important that also the transfer matrix between the APW and a pure plane wave (PW) representation of the wave function is **k** independent. Having obtained the all-electron eigenfunctions, we change to a PW representation, which facilitates the calculation of the matrix elements in Eq. (1).

The element ε_{00} of the dielectric matrix is calculated in the APW representation using the standard formalism for momentum matrix elements.[16] To calculate the matrix elements of the density operator $\langle\mathbf{k}\lambda'|\exp(i\mathbf{G}\mathbf{r})|\mathbf{k}\lambda\rangle$ the wave

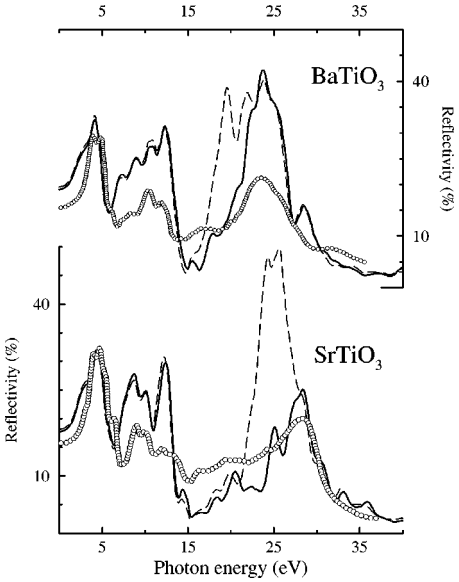

FIG. 3. Reflectivity spectra of $SrTiO_3$ and $BaTiO_3$ with local fields (solid lines) and without local fields (dashed lines). Open circles show reflectivity measurements by Bäuerle *et al.* (Ref. 20) ($\hbar\omega>10$ eV) and by Cardona (Ref. 21) ($\hbar\omega<10$ eV).

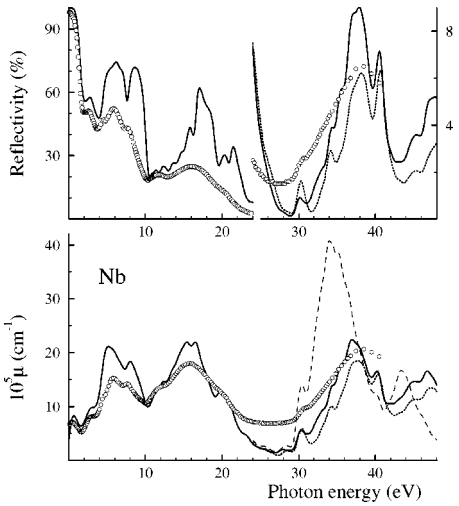

FIG. 4. Reflectivity and absorption coefficient of Nb. Theoretical spectra are shown by solid lines (with LF and XC corrections), dotted lines (with LF but without XC), and a dashed line (without LF). The structure at 30.5 eV marks the onset of transitions from Nb $4p$ band located between -31 and -29.5 eV relative to the Fermi level to the unoccupied part of Nb $4d$ band. Open circles show the experimental data of Weaver *et al.* (Ref. 22) ($0.1<\hbar\omega<36.4$ eV) as tabulated in Ref. 2. The spectrum measured by Truong *et al.* (Ref. 23) ($6.6<\hbar\omega<23$ eV, not presented here) is very close in shape to that of Weaver *et al.*, but their reflectivity values are consistently higher than those of Weaver *et al.* (e.g., near 8 eV: 53% vs 40%; near 20 eV: 25% vs 15%) and agree better with our calculations.

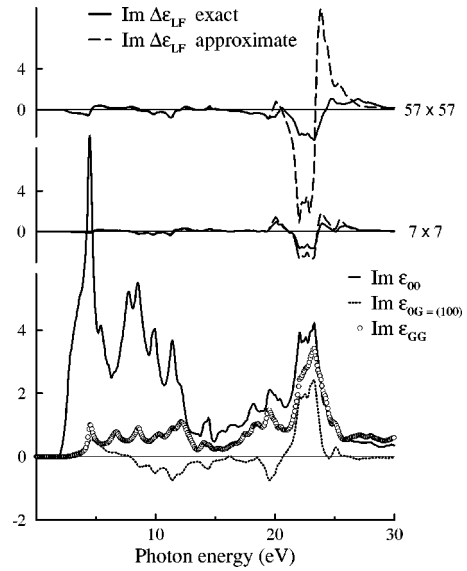

FIG. 5. Lower panel: imaginary part of the dielectric matrix of $SrTiO_3$. The element ε_{00} is shown by a solid line. The diagonal element of the first coordination shell is shown by open circles. The ''wing'' of the dielectric matrix ($\mathbf{G}=0$, $\mathbf{G}'\neq 0$) gives rise to a single independent function (dashed curve). Upper panel: the local field correction to the macroscopic DF by Eq. (2) (solid lines) and by Eq. (3) (dashed lines).

functions $\psi_{\mathbf{k}\lambda}(\mathbf{r})=\langle \mathbf{r}|\mathbf{k}\lambda\rangle$ are expanded in plane waves using the gouging technique described in Ref. 17. Each atom is surrounded by a small sphere of radius R_g inside which the wave function is damped by multiplying $\psi_{\mathbf{k}\lambda}(\mathbf{r})$ by a function $g(r)$ [$g(R_g)=1$; $g(r)$ goes smoothly to zero with $r\rightarrow 0$]. In contrast to the original all-electron wave function, the PW decomposition of the damped function converges very fast, and only a small contribution to the matrix element from the close vicinity of the nuclei is lost. The damped wave functions are then used to calculate the $\mathbf{G}\neq 0$ matrix elements in Eq. (1).

That the above approximation works well is shown by Fig. 1, in which we compare the function $\varepsilon_{00}(\omega)$ of $BaTiO_3$ as given by true wave functions and by damped ones. The radii R_g were 1.4 a.u. for Ba and Sr, 0.4 a.u. for Ti and O, and 0.7 a.u. for Nb. For the perovskites, the PW set comprised all the waves with $G<10.5(2\pi/a)$ (4945 PW's), and for niobium it was $G<16.7(2\pi/a)$ (9861 PW's). The damped wave functions are seen to reproduce the spectrum with a good quality, especially in the far UV region (Ba $5p\rightarrow 5d$ transitions). For niobium the two curves practically coincide (not shown).

To calculate the imaginary part of $\varepsilon_{\mathbf{GG}'}(\omega)$ the integration over the Brillouin Zone (BZ) in Eq. (1) was performed with the tetrahedron method.[19] Both for the perovskites (simple cubic lattice) and for Nb (bcc) we used 286 $\mathbf{k}$ points in the irreducible BZ, which was thereby didvided into 1000 tetrahedra. The real part of $\varepsilon_{\mathbf{GG}'}(\omega)$ was obtained by the Kramers-Kronig analysis.[5] The numerical accuracy of the ELAPW-**kp** method ensured reliable Im $\varepsilon_{\mathbf{GG}'}(\omega)$ functions up to $\hbar\omega_{\max}=50$ eV for the perovskites and up to 70 eV for Nb. These values were taken as upper limits in the Kramers-Kronig integration. For $\varepsilon_{00}(\omega)$, the contribution to the f sum rule from the energy region considered was 98% for Nb but only $\sim$85% for perovskites. For $\mathbf{G}\neq 0$, the spectra are more extended: in the first coordination shell, the integral amounts to 66% of the f sum (Nb) and 68% (perovskites). The discrepancy grows rapidly with increasing $|\mathbf{G}|$. Nevertheless, the ultimate results were stable to the imperfections of the Kramers-Kronig analysis. We checked that by extrapolating diagonal elements $\varepsilon_{\mathbf{GG}}(\omega)$ with slowly decaying tails so as to satisfy the f sum rule.

The band structure was calculated self-consistently within the local density approximation (LDA). The method of constructing the nonmuffin-tin potential and typical computational parameters of the ELAPW-**kp** method are presented elsewhere.[17]

The effects of exchange and correlation (XC) in the induced fields were taken into account within the time dependent adiabatic LDA.[18] The macroscopic DF was obtained by inverting the dielectric matrix of size 57×57 in perovskites and 79×79 in Nb. Figure 2 shows the convergence of the absorption coefficient $\mu(\omega)$ of $SrTiO_3$ with increasing the rank of the dielectric matrix. In perovskites convergence over the entire spectrum was achieved with 27 $\mathbf{G}$ vectors (three coordination shells). The local field effects are seen to be negligible up to the onset of transitions from Sr $4p$ bands at 20 eV. The Sr $4p\rightarrow 5d$ absorption band shifts to higher energies by 3 eV and its maximal intensity decreases by 35%. The neglect of the XC corrections slightly overestimates the effect: the shape of the spectrum remains the same, but the maximal intensity further decreases by $\sim$10%.

The effect of the local fields on the reflectivity is even more dramatic. In Fig. 3 we compare our theoretical spectra

with the reflectance measurements of Refs. 20 and 21. Without local fields the UV part of the spectra is completely incorrect, but the full dielectric matrix yields satisfactory agreement with the measurements. In the low-energy part (0−7 eV) discrepancies are seen, which are presumably due to our neglect of quasiparticle effects. However, the gross features of the spectra are well reproduced by the macroscopic dielectric function.

In metals, the quasiparticle effects are less pronounced, which explains the better agreement with the experiment for Nb (Fig. 4). The LF corrections influence the optical spectra in the same manner as in the perovskites: the far UV absorption band shifts by 3 eV upwards, and the reflectivity in the interval from 30 to 40 eV decreases by a factor of 5. The high-energy reflectivity in Nb is much lower than in the perovskites and the spectrum turns out to be more sensitive to the XC corrections. However, as in the perovskites, the effect brought about by the Hartree local fields predominates.

To understand why the LF corrections should be expected to reduce the UV absorbance let us assume that the nondiagonal elements of the matrix S in Eq. (2) are small as compared to its diagonal elements. Then the matrix S can be inverted analytically and (within the RPA) we have

$$\Delta\varepsilon_{\mathrm{LF}}(\omega)\approx-\sum_{\mathbf{G}\neq 0}\frac{[\varepsilon_{\mathbf{G}0}(\omega)]^2}{\varepsilon_{\mathbf{GG}}(\omega)}. \tag{3}$$

Figure 5 suggests that the approximation is plausible for the $p\rightarrow d$ transitions we consider. For a small 7×7 matrix, the approximate $\Delta\varepsilon_{\mathrm{LF}}$ function is close to the exact result, and even for a large 57×57 matrix the picture is qualitatively correct. In the case of transitions from narrow semicore bands, the functions $\mathrm{Im}\,\varepsilon_{\mathbf{GG}'}(\omega)$ can be represented by Lorentzian curves centered at approximately the same energy, $\hbar\omega_0$ (see Fig. 5). That implies that $\mathrm{Re}\,\varepsilon_{\mathbf{GG}'}(\omega_0)\approx\delta_{\mathbf{GG}'}$, and it follows at once from Eq. (3) that at $\omega\approx\omega_0$ the LF correction to $\mathrm{Im}\,\varepsilon$ is negative. A simple analysis of Eq. (3) suggests that the correction is also negative over a finite energy interval $[\omega_0-\Delta\omega;\omega_0]$. The local-fields-induced decrease of $\mathrm{Im}\,\varepsilon$ seems to be a rather general phenomenon, the neglect of which leads to misinterpretation of experimental UV absorbance spectra.

To summarize, we observe a strong influence of the local fields on the far UV part of the optical spectra of $SrTiO_3$, $BaTiO_3$, and Nb, but a negligible effect over the visible and near UV range. The local fields are strong whenever strong dipole-allowed transitions occur and they tend to shift the absorption band due to semicore excitations to higher energies and to reduce its intensity by more than 50%. The effect is caused by the Hartree contribution to the local fields. The exchange-correlation contribution is important for the accurate description of such excitations: it tends to slightly reduce the effect.

A pronounced disagreement between theoretical results that do not include a full dielectric matrix and experiment in the UV region may produce the impression that a one-electron description of semicore excitations is completely incorrect. On the contrary, our results show that the LDA-based band structure describes semicore states with the same quality as valence states.

We thank O. Krasovska and F. Starrost for helpful discussions. One of the authors (E.E.K.) gratefully acknowledges support by a grant of the Alexander von Humboldt-Stiftung. This work was included in Project No. 05SB8FKA7 supported by the BMBF.

[1] F. C. Brown, in *Solid State Physics*, edited by H. Ehrenreich, F. Seitz, and D. Turnbull (Academic, New York, 1974), Vol. 29.
[2] J. H. Weaver, C. Krafka, D. W. Lynch, and E. E. Koch, *Physics Data, Optical Properties of Metals* (H. Behrens and G. Ebel, Fachinformationszentrum Energie-Physik-Mathematik GmbH Karlsruhe, 1981).
[3] H. Ehrenreich and M. A. Cohen, Phys. Rev. **115**, 786 (1959).
[4] S. L. Adler, Phys. Rev. **126**, 413 (1962); N. Wiser, *ibid.* **129**, 62 (1962).
[5] D. L. Johnson, Phys. Rev. B **9**, 4475 (1974).
[6] P. O. Nilsson, in *Solid State Physics*, edited by H. Ehrenreich, F. Seitz, and D. Turnbull (Academic, New York, 1974), Vol. 29.
[7] F. Aryasetiawan and O. Gunnarsson, Phys. Rev. B **49**, 16 214 (1994).
[8] F. Aryasetiawan, O. Gunnarsson, M. Knupfer, and J. Fink, Phys. Rev. B **50**, 7311 (1994).
[9] F. Aryasetiawan and K. Karlsson, Phys. Rev. Lett. **73**, 1679 (1994); K. Karlsson and F. Aryasetiawan, Phys. Rev. B **52**, 4823 (1995).
[10] H. Bross, O. Belhachemi, B. Mekki, and A. Seoud, J. Phys.: Condens. Matter **2**, 3919 (1990).
[11] M. Ehrnsperger and H. Bross, J. Phys.: Condens. Matter **9**, 1225 (1997).
[12] S. G. Louie, J. R. Chelikowsky, and M. L. Cohen, Phys. Rev. Lett. **34**, 155 (1975).
[13] A. J. Forsyth, T. W. Josefsson, and A. E. Smith, Phys. Rev. B **54**, 14 355 (1996).
[14] V. I. Gavrilenko and F. Bechstedt, Phys. Rev. B **54**, 13 416 (1996).
[15] E. E. Krasovskii and W. Schattke, Phys. Rev. B **56**, 12 874 (1997).
[16] E. E. Krasovskii, V. N. Antonov, and V. V. Nemoshkalenko, Phys. of Metals **8**, 882 (1990).
[17] E. E. Krasovskii, F. Starrost, and W. Schattke, Phys. Rev. B **59**, 10 504 (1999).
[18] S. P. Singhal and J. Callaway, Phys. Rev. B **14**, 2347 (1976); the quality of the adiabatic approximation is discussed by E. K. U. Gross and W. Kohn, Phys. Rev. Lett. **55**, 2850 (1985).
[19] G. Lehmann and M. Taut, Phys. Status Solidi B **54**, 469 (1972).
[20] D. Bäuerle, W. Braun, V. Saile, G. Sprüssel, and E. E. Koch, Z. Phys. B **29**, 179 (1978).
[21] M. Cardona, Phys. Rev. **140**, A651 (1965).
[22] J. H. Weaver, D. W. Lynch, and C. G. Olson, Phys. Rev. B **7**, 4311 (1973).
[23] V. V. Truong, L. J. LeBlanc, and G. J. Turpin, J. Opt. Soc. Am. **68**, 1017 (1978).